doi:10.1111/evo.12501

Shape-shift: Semicircular canal morphology responds to selective breeding for increased locomotor activity

Heidi Schutz,[1,2,3] Heather A. Jamniczky,[4] Benedikt Hallgrímsson,[4] and Theodore Garland Jr.[2]

[1]*Biology Department, Pacific Lutheran University, Tacoma, Washington 98477*

[2]*Department of Biology, University of California, Riverside, California 92521*

[3]*E-mail: schutzha@plu.edu*

[4]*McCaig Institute for Bone and Joint Health, Department of Cell Biology & Anatomy, Cumming School of Medicine, University of Calgary, Calgary, Alberta T2N 4N1, Canada*

Received January 13, 2014
Accepted July 6, 2014

Variation in semicircular canal morphology correlates with locomotor agility among species of mammals. An experimental evolutionary mouse model was used to test the hypotheses that semicircular canal morphology (1) evolves in response to selective breeding for increased locomotor activity, (2) exhibits phenotypic plasticity in response to early-onset chronic exercise, and (3) is unique in individuals possessing the minimuscle phenotype. We examined responses in canal morphology to prolonged wheel access and selection in laboratory mice from four replicate lines bred for high voluntary wheel-running (HR) and four nonselected control (C) lines. Linear measurements and a suite of 3D landmarks were obtained from 3D reconstructions of μCT-scanned mouse crania (μCT is microcomputed tomography). Body mass was smaller in HR than C mice and was a significant predictor of both radius of curvature and 3D canal shape. Controlling for body mass, radius of curvature did not differ statistically between HR and C mice, but semicircular canal shape did. Neither chronic wheel access nor minimuscle affected radius of curvature or canal shape These findings suggest that semicircular canal morphology is responsive to evolutionary changes in locomotor behavior, but the pattern of response is potentially different in small- versus large-bodied species.

KEY WORDS: **Experimental evolution, Voluntary exercise, 3D morphometrics.**

Studying the evolution of locomotor behavior is a complex task because so many body systems are involved in the control and execution of locomotion. In particular, the reconstruction of ancestral locomotor states requires that skeletal material be mined for any potential links between morphology and function. These links involve not only the biomechanics and kinematics of interactions between muscles and bones, but also the mechanisms by which movement is sensed, and subsequently, controlled.

In jawed vertebrates (gnathostomes), the three semicircular canals (lateral, anterior, and posterior) of the inner ear are arranged approximately at right angles to each other in the *x*, *y*, and *z* planes and sense angular velocity in three dimensions. The canals provide information on the following movements: the lateral canal senses mediolateral rotation (yaw), the anterior canal senses dorsal–ventral rotation (pitch), and the posterior canal senses head tilt caused by lateral flexion of the cervical vertebrae (roll), as illustrated in Figure 1. These structures supply information on head position, enabling the production of coordinated and simultaneous adjustments to vision, body position, and movement during locomotion (Goldberg and Fernández 2011). Lampreys (representative of the craniates) have long been described as lacking the lateral canal, a defining feature of the Gnathostomata (Janvier 2007), and thought to have emerged with the diversification of the orthodenticle-homeobox *Otx* genes (Mazan et al. 2000). A major focal point in the study of vertebrate evolution is the elucidation of how complex and diverse locomotor behaviors evolved in this lineage and how skeletal structures (dominating the

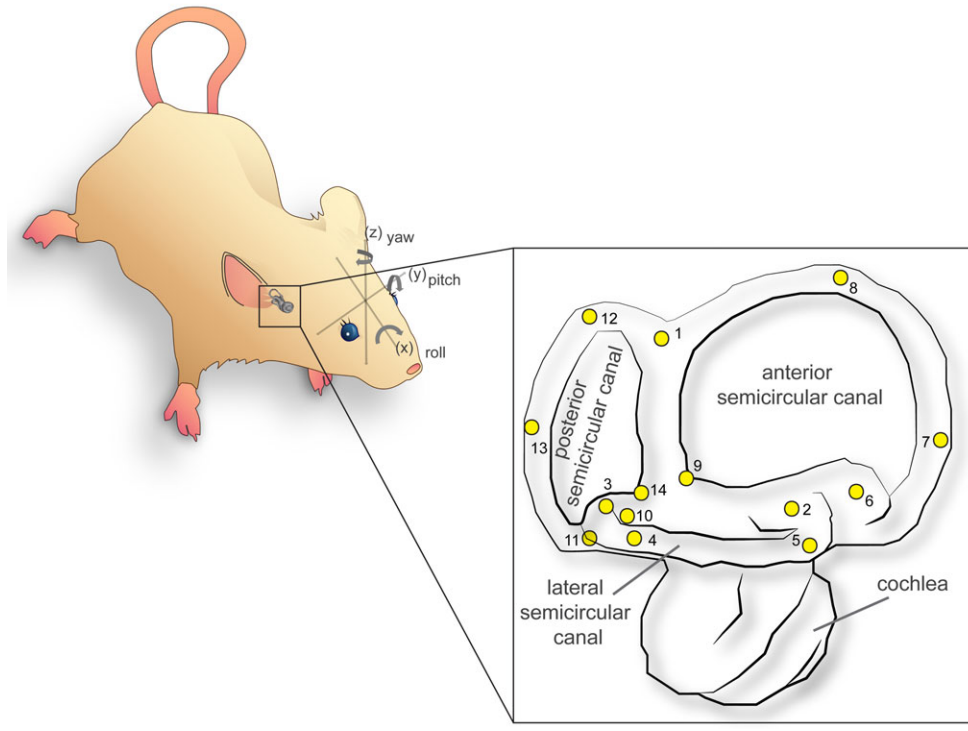

Figure 1. **Anatomical position of the semicircular canals, vestibule, and cochlea in a mouse with an enlarged view of these structures along with three-dimensional landmark configurations of the semicircular canals employed in this study. Fourteen three-dimensional landmarks were placed according to the anatomical descriptions listed and described in Table S1. This figure features a mouse image "Vectorized adaptation of File:Lab_mouse_mg_3263.jpg" by David Liao (2013) used under a Creative Commons Attribution 2.0.**

fossil record) could be used to reconstruct these behaviors. Early on, comparative anatomists suggested that semicircular canal size was associated with locomotor function (Gray 1907, 1908), leading to various efforts directed at quantifying not only this relationship, but any correlation between canal morphology and locomotion. The radius of curvature in particular has repeatedly been shown to correlate with locomotor behavior and "agility," with more agile species tending to have larger canals (Spoor and Zonneveld 1998; Spoor et al. 2007; Walker et al. 2008; Cox and Jeffery 2010). The presence of such patterns opened new avenues of inquiry for the assessment of locomotor function in a diverse group of extinct vertebrates, from primates (Silcox et al. 2009; Ryan et al. 2012) and notoungulates (Macrini et al. 2010) to xenarthrans (Billet et al. 2013). Additional measures of semicircular canal morphology include indicators of the canals' deviation from circularity (Cox and Jeffery 2010), planar and angular characteristics (Blanks et al. 1972, 1975, 1985; Calabrese and Hullar 2006; Hullar 2006; Cox and Jeffery 2008), crosssectional area (Bradshaw et al. 2010), and various descriptors of three-dimensional shape ranging from qualitative (Spoor and Zonneveld 1998) to quantitative (Bradshaw et al. 2010; Cox and Jeffery 2010; Gunz et al. 2012). Like the radius of curvature, many of these measures have also been shown to correlate with locomotor agility. Furthermore, recent work by Gunz et al. (2012) has demonstrated the capacity of shape data to differentiate canal morphology at the subspecies level for *Pan troglodytes*, whereas prior work using size measures showed minimal differences in canal size within the genus *Pan* (Spoor and Zonneveld 1998), thus suggesting that semicircular canal shape may be sensitive to fine-grained phylogenetic differences, or perhaps more subtle differences in locomotor function not detected by canal size measures such as the radius of curvature. The ability for fine-grained differentiation of morphological differences in these structures expands the possibility for comparative study to investigate evolutionary transitions and diversity in the locomotor function of vertebrate lineages.

Many studies have also shown that canal size and some elements of shape exhibit a negatively allometric relationship with body size, with smaller species having relatively larger canals than large species (Spoor et al. 2007; Walker et al. 2008; Silcox et al. 2009; Ryan et al. 2012). However, those studies are broad in phylogenetic scope and encompass large variations in body size and locomotor habits. It has yet to be determined whether negative allometry holds when examining within-species variation (static allometry) and whether small body size constrains or alters canal structure responses to evolutionary changes in locomotor agility.

All of the above-listed studies employed interspecific comparisons, which can identify patterns and characters of interest, but generally provide limited information on evolutionary mechanisms (Swartz et al. 2003; Rezende et al. 2005b; Rezende and Diniz-Filho 2012). Experimental evolutionary models are an excellent complement to comparative studies because they provide opportunities for testing evolutionary hypotheses while allowing for control of numerous extraneous variables (Garland and Rose 2009), such as confounding traits that are correlated with phylogenetic relationships or differences in the life-history status of an individual. They also allow for replication of selected and control lines, enabling separation of the effects of random genetic processes, such as drift, and true correlated responses to selection, as well as variation in the mechanisms of that response, termed "multiple solutions" (Bennett and Lenski 1999; Garland 2003; Garland et al. 2011a).

In this study, we employed an experimental evolutionary approach, and used three-dimensional geometric morphometric techniques to quantify the response of semicircular canal morphology to both selective breeding for high voluntary wheel-running behavior and chronic voluntary exercise on wheels (i.e., possible differences in phenotypic plasticity: Garland and Kelly 2006 and Kelly et al. 2012). The animals used in this study are derived from a selection regime for high voluntary wheel running enforced for 21 generations (the full background of the selection experiment is provided in the Methods and in Appendix S1 of the supplementary information). By generations 16–25, and persisting in later generations, all four replicate selectively bred high-runner (HR) lines had reached selection limits at which the mice ran daily running distances two to threefold greater than those run by mice from the four nonselected (C) lines (Girard et al. 2001; Garland 2003; Middleton et al. 2008a; Rezende et al. 2009; Careau et al. 2013). Mice from the HR lines also ran at higher average and maximal speeds for greater distances, as compared with mice from the C lines (Girard et al. 2001; Rezende et al. 2009). To put these running differences in perspective, it may be useful to note that the running wheels measure 1.12 m in circumference (Swallow et al. 1998) and in this specific study C mice ran an average of 4983 revolutions per day, whereas HR mice ran an average of 9667 revolutions per day. This translates to apparent distances covered of approximately 5.6 km by C mice versus 10.8 km by HR mice daily (Kelly et al. 2006), a difference not reflecting the increased proportion of "coasting" revolutions by HR mice (Koteja et al. 1999).

In addition to changes in running behavior and concomitant physiological responses to selection documented in the HR lines (Garland et al. 2011b), a suite of morphological responses have emerged. For example, HR mice are consistently smaller (body mass and length) than C mice (Swallow et al. 1999), and the mice used in the present study follow this trend. In addition, selective breeding has produced specific skeletal responses, including decreased asymmetry, thickness, and mass of long bones in the hind limb and increased size of femoral heads (Garland and Freeman 2005; Kelly et al. 2006). These considerable behavioral and morphological responses to selection show that mice in the HR lines have developed different locomotor repertoires from C mice, and are, arguably, more "agile" (see Discussion for additional details).

Sustained directional selection has been shown to alter the degree of phenotypic plasticity present in populations of various organisms and across many different traits, indicating that plasticity is evolvable (Pélabon et al. 2010; Hayden et al. 2012). Indeed, several physiological traits, including hematocrit, blood hemoglobin content, cytochrome *c* oxidase and pyruvate dehydrogenase activity in hindlimb muscle, have greater phenotypic plasticity in HR mice than the C mice (Garland and Kelly 2006). However, a study of femur morphometrics found that only one of 19 traits showed statistically differential phenotypic plasticity between the HR and C mice in response to long-term wheel access (Middleton et al. 2008b). Moreover, prior work on various laboratory animals, including rodents, suggests that the cranial region immediately surrounding the semicircular ducts matures faster than other skeletal regions and is highly resistant to remodeling. Given these data, it seemed prudent to examine not only if canal morphology responded to selection for daily levels of locomotor activity but also whether the phenotypic plasticity of the canals exhibited a correlated response.

Some individuals in the founding population of mice (~7%) exhibited the HR_{mini} phenotype. Caused by a Mendelian recessive gene, individuals of the homozygous genotype exhibit an ~50% reduction in the mass of the triceps surae muscle complex and of the entire hindlimb compared to normal individuals (Garland et al. 2002; Houle-Leroy et al. 2003). HR_{mini} phenotype individuals were unknown prior to the start of the breeding experiment, and were therefore randomly assigned among the eight lines. Frequency of the minimuscle phenotype increased drastically in the two HR lines (3 and 6) in which it was ever observed, but the phenotype has been lost in the one C line (5) in which it was detected. Eventually, the minimuscle phenotype went to fixation in HR line 3 and remains polymorphic in HR line 6 (Garland et al. 2002; Middleton et al. 2008a).

Mice exhibiting the minimuscle phenotype (HR_{mini}) have numerous differences in anatomical and physiological traits, as compared with normal HR or C individuals, including reduced body masses, increased heart size, increased aerobic enzymes and glycogen stores in some muscles, and increased fatigue resistance in specific lower leg muscles (Garland et al. 2002; Houle-Leroy et al. 2003; Gomes et al. 2009). In terms of their skeletal characteristics, their femora and tibia–fibulae are significantly longer and thinner, and the femora also exhibit unique microstructural

bone morphologies (Houle-Leroy et al. 2003; Kelly et al. 2006; Middleton et al. 2008a; Wallace et al. 2012). These traits have been postulated to provide advantages for the faster running measured in the HR_{mini} mice versus normal HR mice (Middleton et al. 2008a), but it is currently unknown whether the gene has direct and/or indirect pleiotropic effects on skeletal morphology (Wallace et al. 2012; Kelly et al. 2013; see Discussion).

The presence of HR_{mini} individuals in the sample of mice used for this study provided the additional opportunity to investigate whether the unique morphologies they exhibit in other skeletal regions also extends to bony elements of the vestibular apparatus and to provide additional information on the mechanistic effects of this allele on bone. Finally, they provided an opportunity to examine whether the different locomotor characteristics of HR_{mini} mice (i.e., slight but significantly faster speeds of HR_{mini} versus normal HR mice during voluntary wheel running including the mice in this specific sample [Kelly et al. 2006]) were sufficient to produce responses in semicircular canal morphology.

Given the dramatic differences in voluntary wheel-running behavior and in home-cage activity levels (when mice do not have wheel access) between the HR and C mice (Malisch et al. 2009), the wide array of skeletal differences already observed between them and the known effects of the minimuscle phenotype—all of which are observed in body regions closely associated with locomotor activity—this study system is well-suited to investigations of how semicircular canal morphology varies within a single small-bodied species that displays large variation in locomotor function. Here we test the hypotheses that canal size and/or shape (1) has evolved in response to the selective breeding experienced by the four replicate HR lines, (2) exhibits phenotypic plasticity in response to chronic exercise that begins at a young age, and (3) exhibits a unique morphology in individuals with the minimuscle phenotype.

Materials and Methods

MICE FROM SELECTIVELY BRED LINES

This study used laboratory mice generated by long-term artificial selection for high voluntary wheel-running behavior (see Appendix S1*)*. Eight closed lines are separated into four nonselected C and four HR lines, in which the parents of subsequent generations are those mice that exhibit the highest levels of voluntary wheel running (Swallow et al. 1998; Garland 2003; Careau et al. 2013). A small percentage of the base population exhibited a "minimuscle" (HR_{mini}) phenotype, characterized by an approximate 50% reduction in hindlimb muscle mass (Garland et al. 2002; Houle-Leroy et al. 2003).

The present study used the skeletonized cranial remains of males from a second litter of generation 21 (21b). We examined evolutionary change and phenotypic plasticity of various traits by simultaneously studying the combined effects of selection for voluntary wheel running and wheel access versus deprivation for approximately eight weeks beginning shortly after weaning (Kelly et al. 2006, see Appendix S1).

MICROCOMPUTED TOMOGRAPHY, LINEAR MEASUREMENTS, AND DATA ANALYSIS

The temporal regions of the crania of all individuals were subjected to microcomputed tomography (μCT; Viva-CT40, Scanco Medical AG, Basserdorf, Switzerland) at 21 μm resolution (see Appendix S2). Linear measurements of all three right semicircular canals (anterior, lateral, and posterior) were performed in Amira 5.0 (Visualization Sciences Group, Burlington, MA) following a subset of the measurements described by Spoor and Zonneveld (1995). Specifically, we measured the width and height of each canal and used the means of these measurements to calculate the radius of curvature for each canal per Curthoys et al. (1977, see Appendix S2). We then calculated the mean radius of curvature of all three canals for each individual. Because of the design elements of the selection model and the specific experiment presented herein, we needed to make simultaneous comparisons of canal size between the two line-types (HR vs. C) under two experimental treatments for locomotor activity (wheel access and no wheel access), as well as testing the main effect of the mini muscle phenotype (HR_{mini}). To test if canal size differed between line-types and experimental treatments (fixed effects), the radius of curvature for each canal and the mean radius of curvature were analyzed via two-way ANCOVA in SAS Procedure Mixed (SAS Institute) with type-III tests of fixed effects, with line (1–8) nested within line-type (HR or C) as a random effect, family nested within line as a random effect, mini muscle (HR_{mini}) as a fixed effect, and log body mass as a covariate (see Kelly et al. 2006).

3D LANDMARKS AND SIZE METRICS USED

Three-dimensional landmarking of all three right canals was performed in Amira (see Appendix S3). We partially followed the landmarking scheme of Lebrun (Lebrun et al. 2010), replicating 12 (10–22) of their 22 landmarks and formulating an additional two new landmarks for a total of 14. Landmark definitions and illustrations are shown in Table S1 and Figure 1.

The MorphoJ (v. 1.03a) software package (Klingenberg 2011) was used to perform a geometric morphometric analysis of the 3D coordinate data (see Appendix S3). Prior work suggests that assessment and control of allometric effects can be done by performing a multivariate regression of shape on size (Monteiro 1999; Klingenberg 2010). In a preliminary analysis, Procrustes coordinates were regressed on centroid size and we evaluated the independence between size and the shape variables with a 10,000-round permutation test. After examining results of this

analysis (see Appendix S3), we chose to present and interpret the results of the nonadjusted data. In studies in which size differences among specimens are considerable (e.g., dog skulls in Drake and Klingenberg 2010) and in which centroid size of the element reflects body size closely and allometric effects on shape exist, this adjustment is appropriate. For the dataset presented here, however, size differences among individuals are smaller and they involve numerous metrics of canal size and body size (radius of curvature, centroid size, and body mass) that, although statistically correlated with one another, potentially serve different functions (such as canal size potentially changing with degree of agility).

MANOVA/MANCOVA ANALYSES WITH RANDOM NESTED FACTORS

To compare mean semicircular canal shape between the two line-types under the two experimental treatments, along with the main effect of minimuscle, we performed shape analyses utilizing a limited shape space (eight principal components [PCs] rather than the generated 35). We executed a series of two-way MANCOVAs in SAS Procedure Mixed with type-III tests of fixed effects (line-type and activity), with line (1–8) nested within line-type (HR or C) as a random effect; minimuscle ($HR_{mini)}$ as a fixed effect; and body mass, nose-rump length, or centroid size as a covariate. The standard MANOVA/MANCOVA infrastructure makes random nested factors difficult to accommodate and, as a consequence, we used an alternative MANOVA/MANCOVA technique.

Traditional MANOVA/MANOCVA analyses geared toward the use of fixed effects were incompatible with our experimental set up because the degrees of freedom for the nested term must be equal to or greater than the number of dependent variables. Consequently, as the number of dependent variables increases, the matrix determinant becomes negative. To account for these issues, alternative means of performing MANOVA and MANCOVA analyses with such datasets have been used (Langerhans 2009; Langerhans and Makowicz 2009). In the present dataset, a positive determinant is achieved using eight dependent variables or fewer. In our analyses, we used PCs 1–8, which accounted for 73.2% of the total variance in shape. Just as with the univariate data, our multivariate statistical model must incorporate the designs of both the selection protocol and the specific experiment this set of mice were subjected to. Our comparisons of canal shape must be made simultaneously between the two line-types (HR vs. C) under two experimental treatments for locomotor activity (wheel access and no wheel access), as well as testing the main effect of the minimuscle phenotype (HR_{mini}). To do so, all analyses are performed in SAS Procedure Mixed. However, SAS Procedure Mixed does not accept multiple dependent variables; therefore, the PC scores were treated as repeated measures and a PC "trait" variable identifying each PC was created (Wesner et al. 2011; Hassell et al. 2012). We interpreted the results of the interactions of the PC trait variable with the fixed variables in the model.

BODY MASS AND SIZE METRICS USED

Because allometric shape changes are quite common, the effects of size on shape require identification. In this dataset, various size metrics were collected and before proceeding with data analysis, an assessment of which size variable(s) were most appropriate to include in the analyses was necessary. The results of these preliminary analyses and their biological relevance led us to use body mass as the relevant size metric in all subsequent analyses (see Appendix S4).

Results

NEITHER WHEEL ACCESS NOR SELECTIVE BREEDING AFFECTS SEMICIRCULAR CANAL RADIUS OF CURVATURE

Consistent with results from previous multispecies comparative studies, we found that canal radius of curvature generally scales positively with body mass such that larger mice have larger canals (Table 1, Fig. 2), except for the posterior canal ($P = 0.6051$). As previously reported, the HR mice are smaller, on average, than C mice (Kelly et al. 2006), a finding consistent across multiple generations (Swallow et al. 1999; Rezende et al. 2009; Garland et al. 2011a), and they also display a nonsignificant trend toward absolutely smaller canals than C mice (Fig. 2). However, ordinary least-squares regression (OLS, Fig. 2) indicated that the relationship between canal size and body mass was also negatively allometric, with smaller mice having proportionately larger canals than larger mice. More specifically, isometry of canal radius versus body mass would be indicated by a slope of 1/3, whereas the slopes of OLS regressions between canal size and body mass range from 0.154 to 0.074 (with and without outliers, see Fig. 2). This result parallels the findings of earlier interspecific comparisons (Watt 1924; Jones and Spells 1963; Spoor and Zonneveld 1998; Walker et al. 2008; Silcox et al. 2009; Ryan et al. 2012) showing that smaller species tend to have proportionately larger canals.

After statistically controlling for body mass, the analyses (run with and without outliers, but only results with outliers removed are reported) indicated no significant effect of wheel access or selection history on canal radius of curvature, either individually or averaged (Table 1, Fig. 2). Additionally, the line-type-by-wheel access interaction was never statistically significant (Table 1).

A total of nine mice in the sample were identified as having the minimuscle phenotype, and minimuscle status was not a

Table 1. Significance levels (*P*-values) from two-way nested analysis of covariance models implemented in SAS Procedure Mixed.

Variable	*N*	Wheel Access	Line type	Wheel Access × Line type	Minimuscle	Body Mass
Degrees of freedom		*1, 6*	*1, 6*	*1, 6*	*1, ~29*	*1, ~29*
R of the anterior canal	78	0.2528+	0.7083−	0.2410	0.3421+	**0.0004+**
R of the lateral canal	80	0.7479+	0.9250+	0.5816	0.2484+	**0.0489+**
R of the posterior canal	78	0.9782+	0.3625−	0.5733	0.4601+	0.6051
Mean *R* for all three canals	77	0.5428+	0.9522−	0.3881	0.4478+	**0.0228+**

Line type (HR or C with + indicating that mice from the HR lines have larger measurements and – indicating smaller measurements) and wheel access (+ indicating that mice housed with access to running wheels because weaning at 21 days of age have larger measurements, – indicates smaller measurements) were the two main grouping factors and considered fixed effects. The effects of wheel access and the wheel access by line-type interaction were tested over the mean squares of the wheel access by line (8) interaction and all were tested with 1 and 6 df. The main effect of the minimuscle phenotype (+ indicating that minimuscle mice have larger measurements and – indicating that they have smaller measurements) was also included in the model and was tested over the mean square error and body mass was included as a covariate: both were tested with 1 and 29 df (or fewer depending on outlier removal).
Bold indicates $P < 0.05$, unadjusted for multiple comparisons and R = radius of curvature.

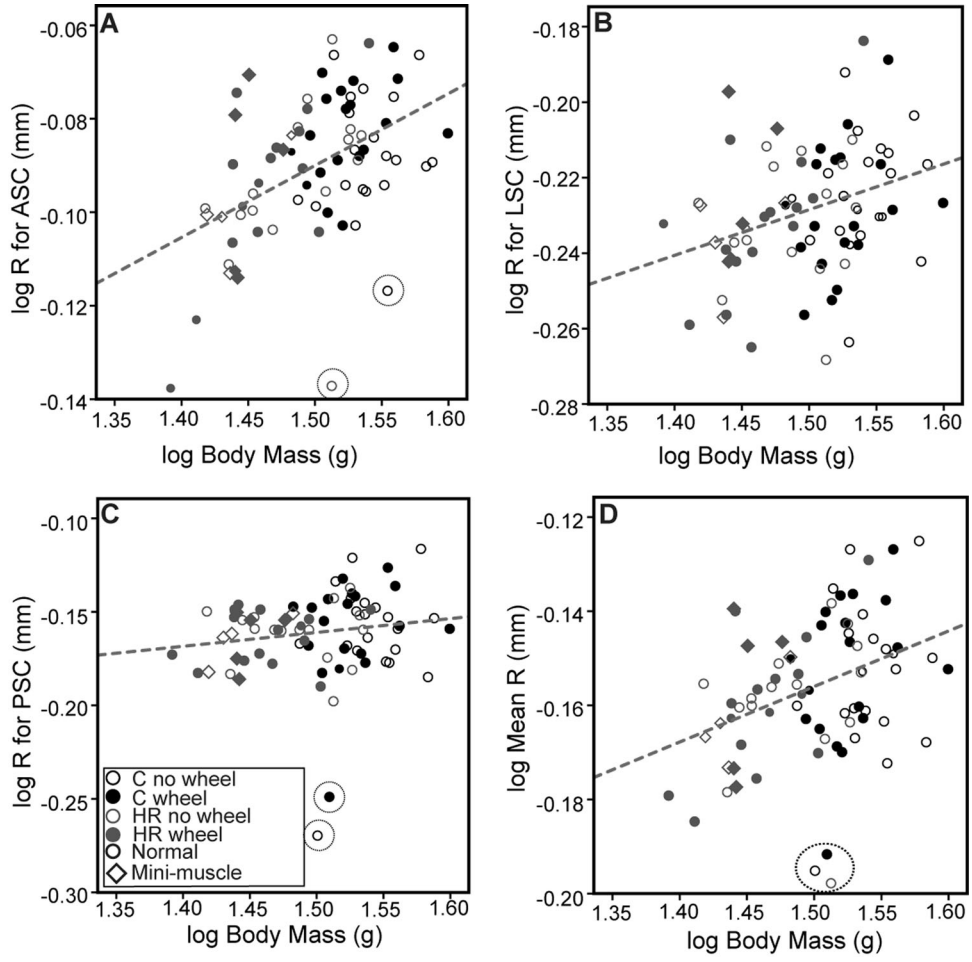

Figure 2. Relationship between log body mass and (A) log anterior semicircular canal (ASC) radius of curvature, (B) log lateral semicircular canal (LSC) radius of curvature, (C) log posterior semicircular canal radius of curvature (PSC), and (D) the log mean radius of curvature of all three canals for four experimental groups of 80 mice with outliers included (see text). The dashed lines represent the simple least-squares linear regression (with outliers included and identified by the black circles with dotted lines) with the values of the intercepts and slopes as follows: A:slope = 0.154, intercept = −0.321; B:slope = 0.121, intercept = −0.410; C:slope = 0.074, intercept = −0.272; D:slope = 0.118, intercept = −0.333. Values when outliers were removed were as follows: A:slope = 0.127, intercept = −0.419; B:no outliers, values same as above; C:slope = 0.080, intercept = −0.278; D:slope = 0.124, intercept = −0.341. ANOVAs (see Table 1) were performed on either the full dataset or with removal of outliers.

statistically significant predictor of any of the radii of curvature, nor their cumulative mean (Table 1).

SELECTION REGIME STRONGLY AFFECTS SEMICIRCULAR CANAL SHAPE

In contrast to the analyses of canal radius with body mass as a covariate, selection history had a highly significant effect on canal shape (Table 2). Aside from this effect, the mixed-model nested MANCOVA indicated no significant effects of body mass (allometry), minimuscle, wheel access (the experimental treatment), or the interaction between wheel access and selection history (line type). Figure 3 depicts the shape variation in the dataset as described by the first three PCs, which account for 44.6% of the total shape variation. Separation between HR and C mice is seen along all three axes, but group separation is most pronounced on PC1 (see Fig. 3A, B and Appendix S5 for a full description of morphological differences).

Table 2. Nested multivariate analysis of covariance (MANCOVA) models examining overall shape variation of the three semicircular canals (uniform components and partial warps) using body mass as a covariate.

Effect	df	*F*	*P*
Wheel access	7, 42	0.20	0.9828
Line type	7, 42	3.62	**0.0039**
Minimuscle	7, 462	1.34	0.2272
Activity × line type	7, 42	0.46	0.8609
Body mass	1, 462	0.08	0.7737

Similar models were run using nose-rump length, or centroid size as a covariate, but are not shown here because they are similar to those using body mass as a covariate. Analyses were performed as repeated measures for eight PCs of a total of 35 possible, and the results below are for the interactions between a formulated PC trait variable with eight levels (for each PC used in the analysis) and the fixed effects in the model. Bold indicates a significant result at the $P < 0.05$ level.

Discussion

Selective breeding for high voluntary wheel-running behavior in house mice has had differential effects on the shape and size of the semicircular canals. Canal shapes, as measured using three-dimensional geometric morphometrics, are significantly different between the selectively bred HR and nonselected C lines of mice. In contrast, canal size (adjusted for variation in body size) revealed no differences between HR and C mice.

We propose that the observed changes in canal morphology result from the low phenotypic plasticity of the semicircular canals (as evidenced by the present study, which resulted in the absence of any effect of being housed with wheels), coupled with the manner in which the canals respond to important but comparatively small (relative to differences observed among species) evolutionary changes in locomotor behavior that do not necessarily, or perhaps only very subtly, alter gait. Further, the lack of differences in canal size between the HR and C mice may be attributable to either (1) constraints placed on semicircular canal enlargement by the small temporal bones found in small bodies or (2) the fact that at an absolutely smaller canal size in a smaller body may provide different biomechanical responses to agile locomotor behaviors. Taken together, our results indicate that a different evolutionary solution may be required in small-bodied species as a response to increases in locomotor agility, and this outcome may have implications for the study of locomotor behavior across vertebrates.

SEMICIRCULAR CANALS ARE NOT AFFECTED BY THE MINIMUSCLE PHENOTYPE

The mice used in this study that expressed the minimuscle phenotype not only ran faster than normal HR individuals, but also showed specific femoral and tibiofibular proportions (Kelly et al. 2006) along with differences in their femoral cortical morphology (Wallace et al. 2012). The mechanisms by which these minimuscle effects arise remain unknown, but Wallace et al. (2012) suggest several possibilities, including direct pleiotropic influences of the minimuscle allele on bone, secondary mechanical responses caused by the effects of the gene on muscle mass and contractile properties, or differences in circulating hormonal or growth factor concentrations caused by the allele. Our results indicate, however, that the minimuscle phenotype does not influence all aspects of skeletal morphology.

We found no statistical effects of the minimuscle trait on a suite of canal measurements. Although these results do not definitively pinpoint the mini-muscle allele's mode of action, the fact that its influence is absent in this region suggests that its effects are not universal across all skeletal structures. Unlike the appendicular skeleton, the vestibular apparatus, although functionally associated with locomotion, is not under the direct influence of locomotor muscles. This, in association with a relatively rapid ontogenetic trajectory and resistance to remodeling effects in adulthood, is likely to limit any indirect functional responses to the minimuscle phenotype in this region.

Although minimuscle individuals do exhibit significantly faster wheel-running speeds than normal HR individuals (Syme et al. 2005; Kelly et al. 2006; Dlugosz et al. 2009), the difference is potentially insufficient to produce an effect, particularly because they do not always run farther on a daily basis (Syme et al. 2005; Dlugosz et al. 2009). In addition, speed is only one component of agility (a three-dimensional effect) and may not be enough to alter characteristics of canal morphology through phenotypic plasticity. Finally, we must keep in mind that the number of minimuscle individuals in our sample was small and they were

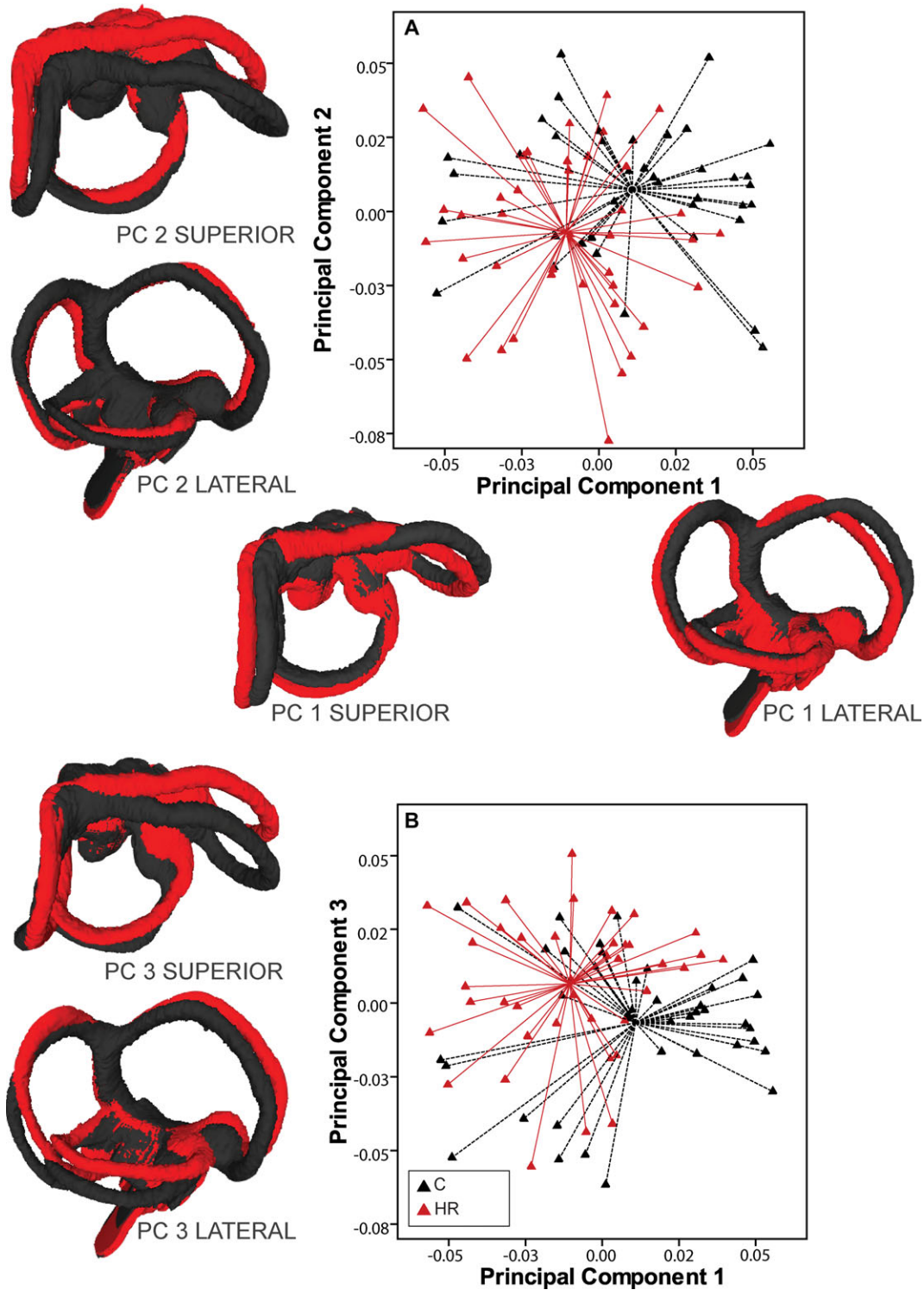

Figure 3. Principal component (PC) analysis for semicircular canal shape in a dataset of 80 mice. (A and B) plots of the PC scores with PC 1 explaining 18.3% of the total shape variation, PC 2 explaining 14.2% of the total shape variation, and PC 3 explaining 12.1% of the total shape variation. The dashed black and solid red lines lead to the group centroid for either HR or C individuals regardless of activity group or minimuscle. Shape changes associated with the positive and negative extremes of each of the PC axes are shown in both lateral and superior views, where the extremes at each PC are overlaid on one another to illustrate shape differences. Each model of semicircular canal shape change is color-coded like the scatter-plots for the group (HR in red, and C in black) that primarily lies in either the positive or negative end of that specific axis. For example, for PC 1, HR individuals (red symbols and models) primarily occupy the negative shape space, whereas C (black symbols and models) individuals occupy the positive one. In contrast, for PC 3, HR individuals occupy the positive space, whereas C individuals occupy the negative space.

also split between two activity treatment groups. Therefore, it is possible that our sample size was too small to allow detection of subtle effects.

SEMICIRCULAR CANALS ARE PHENOTYPICALLY STABLE

Along with the effects of the minimuscle allele discussed above, previous work shows that wheel access also had a number of effects on the hindlimb bone morphology of this specific sample of mice. Regardless of line type, significant differences in body mass and femoral cortical morphology were observed between mice housed with and without wheel access (for eight to nine weeks beginning shortly after weaning, Wallace et al. 2012). These responsive changes to bone microstructure during a critical developmental period prompted us to use to investigate whether such plasticity might be possible in the semicircular canals.

The bony elements of the inner ear reach adult-like proportions much earlier than the appendicular skeleton in most mammals, and the morphology appears to remain stable thereafter, particularly after ossification of the petrosal bone surrounding the canals. Ossification can occur prior to birth, as observed in humans and rabbits (Hoyte 1961; Jeffery and Spoor 2004), early in postnatal development (within a few days of birth) as in rats (Curthoys 1981), or somewhat later (~20 days) as in some marsupials (Clarke 2001; Sánchez-Villagra and Schmelzle 2007; Ekdale 2010). Studies performed on house mice show that the semicircular endolymphatic ducts assume their mature shape and nearly adult size prior to birth and then change only minimally up to postnatal day 6 (Lim and Anniko 1985; Morsli et al. 1998). Specifically, the morphology of the semicircular ducts assumes its mature shape by 15 days postcoitum (Morsli et al. 1998). Consequently, by the time the mice in this study were subjected to the experimental treatment of having access to wheels or not at 25–28 days or age, their canals were likely fully formed.

In addition, bone remodeling in the mammalian otic capsule (which contains the semicircular canals) appears to occur at a much-reduced rate compared with that of other skeletal regions and elements (Sørensen et al. 1990a, 1990b, 1991, 1992), possibly inhibited by significant differences in cytokine system components involved in the molecular mechanisms of bone turnover (Zehnder et al. 2005, 2006). This difference suggests that the components of the otic capsule have limited phenotypic plasticity once adult size and proportions are reached.

We hypothesized that the degree of directional selection experienced by these mice might affect the magnitude of phenotypic plasticity they exhibit and as a consequence produce not only different canal morphologies between the HR and C mice, but also cause the HR mice to experience differential responses to wheel exposure than exhibited by C mice. However, although prior work indicates that differential plasticity of various physiological traits is present (Garland and Kelly 2006) and that differential responses to wheel exposure are present in some skeletal elements of the HR versus C mice (Middleton et al. 2008b; Young et al. 2009), the conserved remodeling physiology of this region apparently prevents similar responses in the semicircular canals.

Given the prior work on remodeling in this region, it seemed unlikely that these specific mice would be any different in their patterns of canal development. Nonetheless, the existence of plasticity differences in other skeletal regions of these mice and the multiplicity of interactive elements available in this sample (selection, the minimuscle allele, and wheel/no wheel experimental treatments) demanded that we investigate how conserved the remodeling mechanism in this region truly was.

SEMICIRCULAR CANAL SHAPE BUT NOT SIZE IS INFLUENCED BY SELECTION FOR INCREASED VOLUNTARY WHEEL RUNNING

Attempts to elucidate the relationship between sensitivity of the vestibular sensory system and canal morphology have demonstrated a relationship between canal size and degree of afferent sensitivity (Hullar 2006; Yang and Hullar 2007; Lasker et al. 2008). In mice, extracellular vestibular nerve recordings show rotational and head velocity sensitivities that are potentially lower than in comparable studies of larger-bodied species. Previous workers hypothesized that these differences were due to the absolutely smaller size of the semicircular canals in smaller species.

As predicted, tests of sensory sensitivity in the semicircular canals of mice show that they are three to four times less sensitive to head rotational movements than larger species (Lasker et al. 2008). Based on mathematical models of fluid movements in ducts, the level of sensitivity (as measured by afferent firing rate) is a function of the radius of the canal. Thus, the reduction in sensitivity is thought to relate to canal size because smaller canals have proportionally smaller amounts of endolymph (a filtrate of the blood) moving in the semicircular ducts relative to the amount of angular velocity of the head (Lasker et al. 2008). When these mathematical models were used to predict values of sensitivity and these values were subsequently compared to the measured sensitivities in mice and other mammalian species (rhesus monkey, chinchilla, and cat), the results were similar. Thus, equivalent head movements in species of varying body size potentially produce different vestibular afferent firing rates and canal size is a way of moderating sensitivity. Analyses of three-dimensional landmark data showed statistically significant differences in canal shape between the HR and C mice, despite a failure to differentiate them based on centroid size or radius of curvature alone.

As discussed above, the components of the otic capsule are not subject to the normal levels of remodeling seen in most other

mammalian skeletal structures. In fact, it has been proposed that this lack or reduction of environmental effects on mature structures of the osseous labyrinth produces considerable phenotypic stability, leading to the representation of genotypes at a very high fidelity (Jeffery and Spoor 2004). Consequently, it may be surmised that radius of curvature measures, although useful when making crossspecies comparisons, lacks the resolution to differentiate among groups within species, at relatively fine phylogenetic scales, even though other morphological differences may be present.

Another explanation may lie in the potentially differential responses at different body sizes. As reported in the Results, although we found no differences in canal size between the HR and C lines when using body size as a covariate, the results of our OLS regressions (Fig. 2) demonstrate a persistent pattern of negative allometry in the sample, such that smaller individuals (which are primarily represented by the HR mice) have absolutely smaller but proportionately larger canals than larger (primarily represented by C mice) individuals.

Jones and Spells (1963) argued that large canals are evolutionary result of both large body size (as larger species move their heads more slowly) and increased agility. This results in a scenario in which the largest canals might be found in taxa that have both a large body size and high agility, and whereby small and agile species may actually benefit more from their absolutely smaller canals—regardless of the negatively allometric patterns seen across lineages. This scenario hinges on the reductions in sensitivity required by the proportionally faster moving heads of small taxa. This potential incongruity in canal size patterns is rooted in the fact that sensing endolymph volume displacement in the semicircular duct is affected by many factors, only one of which is the size (or more specifically, the length as measured by the radius of curvature) of the semicircular canals. Other important factors include the crosssectional area of the ampulla (which contains the actual mechanoreceptive structure, the cupula), the area enclosed by the semicircular canal (which can vary depending on canal shape), and the crosssectional area of the endolymphatic duct, all of which are positively correlated with body mass but which may not change uniformly as body mass changes (i.e., have different allometric relationships; David et al. 2010).

Subtle, but detectable differences in semicircular canal shape have, however, been reported between two closely related primate species with slight differences in locomotor repertoires (Gunz et al. 2012). Here, we were able to differentiate between groups that share considerably greater genetic similarity and probably exhibit even smaller differences in locomotor behavior than the species included in the interspecific comparisons, especially given the limited physical environments of laboratory mice as compared with animals in the wild. It is possible, that one of the reasons for the increased ability of shape data to differentiate among groups is the ability of these methods to (albeit roughly) pick up some of the individual contributors (discussed above) to overall semicircular canal system function.

Examinations of canal morphology figure prominently in the study of primate locomotor patterns (Spoor et al. 2007; Walker et al. 2008). A set of those investigations have specifically focused on the link to the hominin transition to bipedality (Spoor et al. 1994, 1996; Spoor 2003). In fact, some have interpreted changes in the canal morphology of hominins as a component of the evolution of human endurance running (Bramble and Lieberman 2004; Lieberman et al. 2009), and head movement during locomotion may be a large contributor to evolutionary changes in canal morphology

In humans (part of the group that has received the most study), increased running speeds produce faster frequencies of head oscillations, which correlate with increases in the firing rates of sensory neurons and rates of eye and head movements (Grossman et al. 1988; Hirasaki et al. 1999). The relationship between the speed of ocular reflexes and adjustments to head position is thought to be a mechanism for maintenance of gaze stability (Mulavara and Bloomberg 2003). During normal locomotor behavior (walking, running, and jumping), these systems maintain constant head position even while the other body regions increase in movement (Pozzo et al. 1990). It has been shown that as running speed increases (resulting in concomitant increases in head oscillation frequency), the capacity to compensate and maintain a steady gaze drops. However, under ecologically relevant conditions, function of the system does not appear hindered as blurred vision is elicited only in laboratory conditions in which voluntary and repeated head oscillations exaggerate those that occur during normal running and walking (Takahashi et al. 1989).

Although only measured in humans, it is likely that other mammals experience similar types of oscillations and perturbations during locomotion, and it has been postulated that smaller-bodied species experience greater (relative to body size) limb (and potentially greater head) oscillations during locomotion than larger species that tend to have slower head movements (Jones and Spells 1963; Spoor 2003). Essentially, larger species tend to move their heads more slowly than smaller species. These predictions are somewhat supported by limited comparative kinematic data, which suggest that body size considerably affects limb displacement and joint movement, such that smaller species experience greater general limb mobility than do large species (Fischer et al. 2002; Fischer and Blickhan 2006). Further support is provided by the fact that both in the presence and absence of sensory input to the semicircular canal system, mice are capable of maintaining stable head orientations during static posture (Vidal et al. 2004). However, when running, only mice with intact functional semicircular canals appear able to preserve a stable

head orientation and stable locomotor trajectories (Vidal et al. 2004).

These results illustrate the critical aspects of vestibular sensory inputs during locomotor activity and lend further support to the notion that rapid locomotor behaviors likely increase demand on the system and the manner in which that demand occurs is correlated to body size. Thus, the larger semicircular canals of large species (which tend to move their heads more slowly) produce greater sensitivities and the smaller canals of small species (which tend to move their heads more rapidly) reduce sensitivity preventing an overload of the system.

As discussed previously, the shorter but faster running bouts of the HR mice previously reported (Girard et al. 2001; Rezende et al. 2009), as well as the higher mean and maximal running speeds of HR mice in general and specifically shown in the HR mice in this sample (Kelly et al. 2006) result not only in an overall increase in wheel running, when compared to C mice, but potentially demand decreased vestibular system sensitivity both due to increased amounts of agile behavior and reduced body size relative to C mice.

Differences in the average (and maximum) running speeds and duration of wheel running (Girard et al. 2001; Rezende et al. 2009), as well as differences in bout characteristics (Girard et al. 2001), indicate that artificial selection has fundamentally affected the way in which mice run. Additionally, these behavioral differences in locomotion coupled with the various morphological differences observed in the appendicular skeletal elements of HR versus C mice (Rezende et al. 2005a; Kelly et al. 2006; Middleton et al. 2008a,b, 2010; Wallace et al. 2012) indicate potential differences in gait kinematics (although this has not been examined). Consequently, the only established differences that would be expected to affect the evolution of semicircular canal morphology in the HR mice are the overall increases in wheel-running speed (greater average and maximal running speeds [Kelly et al. 2006]) and the shorter and more frequent bouts of running (Girard et al. 2001; Rezende et al. 2009), which result in more acceleration and deceleration events.

CONSTRAINTS ON MORPHOLOGICAL CHANGE OF SEMICIRCULAR CANALS

If, as some of the available data suggest, smaller mammals actually experience greater levels of head acceleration for similar locomotor activities, as compared with larger mammals (Spoor 2003), then reductions in sensitivity may be necessary to prevent overstimulating the system. The question is how do small mammals with already large canals for their body size (Jones and Spells 1963; Spoor and Zonneveld 1998; Spoor et al. 2007) adjust to evolutionary increases in locomotor agility, given the limitations on an increase in canal size and the tendency for proportionately rapid head movements?

Cox and Jeffery (2010) examined how deviations from circularity correlate with body size and agility. They hypothesized that because smaller-bodied species have proportionately larger canals (i.e., the allometric scaling exponent for canal radius versus body mass is $<1/3$), and canal size increases are limited by cranial space, adaptations to increased agility might produce deformations of the canals that cause deviations from coplanarity, rather than simple increases in canal size. The implication of this hypothesis is that measurement of canal size potentially misses a great deal of relevant morphological information because only a small subset of the structure is sampled. To test this hypothesis, Cox and Jeffery (2010) measured canal torsion (deviations from circularity of each canal) as mean angular deviation of three-dimensional landmarks sampled along each canal from a calculated plane of best fit. They found that canal torsion varies little across a comparative sample of mammalian species, and appears to have no relationship with body size. However, they note that their methodology is not particularly sensitive and requires pronounced deviations to register a difference.

By contrast, we were easily able to measure statistically significant differences in canal shape across multiple planes, even in the absence of differences in canal size. As discussed above, this suggests that variation in canal sensitivity may be initially adjusted by shape differentiation and that in situations in which other constraints (such as small body size) limit the ability to alter canal size, changes in canal shape may play a more prominent role than previously thought. In addition, and perhaps more likely, is the argument that modulation of sensitivity in the sensory apparatus housed in the semicircular canals is multifactorial and involves not just one aspect of canal morphology such as size and their angular relationships as described above, but other factors, such as the sizes of the canal area, the ampullae, and the semicircular ducts inside the canals, which together provide a more holistic view of canal morphology (David et al. 2010; Davies et al. 2013). Consequently, although prior research has shown that large canals are associated with increased locomotor agility we believe that continued study of this region may benefit from a return to the comparative data to examine variation of semicircular canal morphology across locomotor agility levels at small body sizes.

Finally, it is also possible that the potential constraints limiting canal size in favor of shape changes are related not only to body size, but also to changes in brain size, which may ultimately affect the geometry of the canals. The relationship between brain size and the shape of the basicranium, which houses the petrous temporal and the semicircular canals, has been explored in different contexts. A variety of studies have indicated that changes in endocranial volume have substantial effects on basicranial shape (Ross and Ravosa 1993; Hallgrímsson et al. 2007; Lieberman

et al. 2008; Bastir et al. 2010). Recent work on the mouse lines studied here has shown that HR mice have relatively heavier brains and larger midbrain volumes than C mice (Kolb et al. 2013), hinting at an important role for brain size in structuring skull variation. Although small body size is associated with proportionately larger canals, changes in overall canal morphology (size and shape) may be also be constrained by a more complex set of factors, including brain size, or as has been previously shown in bats, enlargement of other structures in the same region, such as the cochlea (Davies et al. 2013), and these constraints may again be greater at the lower body size ranges. As a consequence, future comparative, experimental, and developmental studies of semicircular canal morphology should consider the influence of brain size and morphology of all structures of the otic region.

Conclusions and Future Directions

We have demonstrated that three-dimensional analysis of semicircular canal shape, as an integrated mechanism with the three canals serving as interdependent components, is a useful way of accounting for numerous sources of morphological variation present in this structure when assessing the correlation of canal morphology with locomotor behavior. Canal function may be affected not only by individual changes in the shape of each canal, but also by higher-level synergistic changes that affect the three-dimensional shape of the entire system.

Thus, despite the existence of constraints on adult phenotypic plasticity, which stabilize the morphology of this structure throughout life, our results on a large sample of individuals from a single species show that changes in locomotor behavior over a relatively small number of generations exert considerable evolutionary influence on canal morphology. The implications of this work are considerable with regard to the usefulness of 3D canal morphology in the reconstruction and potential differentiation of locomotor behaviors between closely related fossil species and particularly between time sequences showing progressive changes in locomotor behaviors over time. Our results suggest that morphological differences in canal shape are most likely the result of evolutionary change and not within-lifetime remodeling in response to activity levels.

Further work is needed to determine how numerous factors (e.g., body size, variation in the various components of the semicircular canal system, the entirety of the bony labyrinth, brain size, strength of selection, developmental differences) interact to influence whether changes occur in the shape and/or size of the semicircular canals. However, current research on this structure continues to reveal not only the complexity of mechanisms affecting its morphology but also the structure's capacity to reflect nuanced differences in locomotor behavior.

ACKNOWLEDGMENTS

The authors thank Jacinda Larson for generating morphs and Wei Liu for scanning assistance. This study was supported by a U.C. Riverside Chancellor's Postdoctoral Fellowship to HS, Canadian Foundation for Innovation grant to BH, and NSF grant and IOS-1121273 to TG. The authors declare no conflicts of interest.

DATA ARCHIVING

The doi for our data is 10.5061/dryad.3sv4p.

LITERATURE CITED

Bastir, M., A. Rosas, C. Stringer, J. Manuel Cuétara, R. Kruszynski, G. W. Weber, C. F. Ross, and M. J. Ravosa. 2010. Effects of brain and facial size on basicranial form in human and primate evolution. J. Hum. Evol. 58:424–431.

Bennett, A. F., and R. E. Lenski. 1999. Experimental evolution and its role in evolutionary physiology. Am. Zool. 39:346–362.

Billet, G., D. Germain, I. Ruf, C. de Muizon, and L. Hautier. 2013. The inner ear of Megatherium and the evolution of the vestibular system in sloths. J. Anat. 223:557–567.

Blanks, R. H. I., I. S. Curthoys, and C. H. Markham. 1972. Planar relationships of semicircular canals in the cat. Am. J. Physiol. 223:55–62.

———. 1975. Planar relationships of the semicircular canals in man. Acta Otolaryngol. 80:185–196.

Blanks, R. H. I., I. S. Curthoys, M. L. Bennett, and C. H. Markham. 1985. Planar relationships of the semicircular canals in rhesus and squirrel monkeys. Brain Res. 340:315–324.

Bradshaw, A., I. Curthoys, M. Todd, J. Magnussen, D. Taubman, S. Aw, and G. Halmagyi. 2010. A mathematical model of human semicircular canal geometry: a new basis for interpreting vestibular physiology. J. Assoc. Res. Otolaryngol. 11:145–159.

Bramble, D. M., and D. E. Lieberman. 2004. Endurance running and the evolution of *Homo*. Nature 432:345–352.

Calabrese, D., and T. Hullar. 2006. Planar relationships of the semicircular canals in two strains of mice. J. Assoc. Res. Otolaryngol. 7:151–159.

Careau, V., M. E. Wolak, P. A. Carter, and T. Garland Jr. 2013. Limits to behavioral evolution: the quantitative genetics of a complex trait under directional selection. Evolution 67:3102–3119.

Clarke, A. H. 2001. Perspectives for the comprehensive examination of semicircular canal and otolith function. Biol. Sci. Space 15:393–400.

Cox, P. G., and N. Jeffery. 2008. Geometry of the semicircular canals and extraocular muscles in rodents, lagomorphs, felids and modern humans. J. Anat. 213:583–596.

———. 2010. Semicircular canals and agility: the influence of size and shape measures. J. Anat. 216:37–47.

Curthoys, I. S. 1981. The development of function of primary vestibular neurons. Pp. 425–461 *in* R. Romand and R. Marty, eds. Development of auditory and vestibular systems. Academic Press, New York.

Curthoys, I. S., R. H. I. Blanks, and C. H. Markham. 1977. Semicircular canal radii of curvature (R) in cat, guinea pig and man. J. Morphol. 151:1–15.

David, R., J. Droulez, R. Allain, A. Berthoz, P. Janvier, and D. Bennequin. 2010. Motion from the past. A new method to infer vestibular capacities of extinct species. C. R. Palevol 9:397–410.

Davies, K. T. J., P. J. J. Bates, I. Maryanto, J. A. Cotton, and S. J. Rossiter. 2013. The evolution of bat vestibular systems in the face of potential

antagonistic selection pressures for flight and echolocation. PLoS One 8:e61998.

Dlugosz, E. M., M. A. Chappell, D. G. McGillivray, D. A. Syme, and T. Garland. 2009. Locomotor trade-offs in mice selectively bred for high voluntary wheel running. J. Exp. Biol. 212:2612–2618.

Drake, A. G., and C. P. Klingenberg. 2010. Large-scale diversification of skull shape in domestic dogs: disparity and modularity. Am. Nat. 175:289–301.

Ekdale, E. G. 2010. Ontogenetic variation in the bony labyrinth of *Monodelphis domestica* (Mammalia: Marsupialia) following ossification of the inner ear cavities. Anat. Rec. 293:1896–1912.

Fischer, M. S., and R. Blickhan. 2006. The tri-segmented limbs of therian mammals: kinematics, dynamics, and self-stabilization—a review. J. Exp. Zool. A Comp. Exp. Biol. 305A:935–952.

Fischer, M. S., N. Schilling, M. Schmidt, D. Haarhaus, and H. Witte. 2002. Basic limb kinematics of small therian mammals. J. Exp. Biol. 205:1315–1338.

Garland, T. Jr. 2003. Selection experiments: an under-utilized tool in biomechanics and organismal biology. Pp. 23–56 *in* V. L. Bels, J.-P. Gasc, and A. Casinos, eds. Vertebrate biomechanics and evolution. BIOS Scientific Publishers Ltd, Oxford, U.K.

Garland, T. Jr., and P. W. Freeman. 2005. Selective breeding for high endurance running increases hindlimb symmetry. Evolution 59:1851–1854.

Garland, T. Jr., and S. A. Kelly. 2006. Phenotypic plasticity and experimental evolution. J. Exp. Biol. 209:2344–2361.

Garland, T. Jr., and M. R. Rose, eds. 2009. Experimental evolution: concepts, methods, and applications of selection experiments. University of California Press, Berkeley, CA.

Garland, T. Jr., M. T. Morgan, J. G. Swallow, J. S. Rhodes, I. Girard, J. G. Belter, and P. A. Carter. 2002. Evolution of a small-muscle polymorphysm in lines of house mice selected for high activity levels. Evolution 56:1267–1275.

Garland, T. Jr., S. A. Kelly, J. L. Malisch, E. M. Kolb, R. M. Hannon, B. K. Keeney, S. L. van Cleave, and K. M. Middleton. 2011a. How to run far: multiple solutions and sex-specific responses to selective breeding for high voluntary activity levels. Proc. R. Soc. B Biol. Sci. 278:574–581.

Garland, T., H. Schutz, M. A. Chappell, B. K. Keeney, T. H. Meek, L. E. Copes, W. Acosta, C. Drenowatz, R. C. Maciel, G. van Dijk, et al. 2011b. The biological control of voluntary exercise, spontaneous physical activity and daily energy expenditure in relation to obesity: human and rodent perspectives. J. Exp. Biol. 214:206–229.

Girard, I., M. W. McAleer, J. S. Rhodes, and T. Garland Jr. 2001. Selection for high voluntary wheel-running increases speed and intermittency in house mice (*Mus domesticus*). J. Exp. Biol. 204:4311–4320.

Goldberg, J. M., and C. Fernández. 2011. The vestibular system. Pp. 977–1022 in comprehensive physiology supplement 3: handbook of physiology, the nervous system, sensory processes. American Physiological Society, Washington, DC.

Gomes, F. R., E. L. Rezende, J. L. Malisch, S. K. Lee, D. A. Rivas, S. A. Kelly, C. Lytle, B. B. Yaspelkis, and T. Garland. 2009. Glycogen storage and muscle glucose transporters (GLUT-4) of mice selectively bred for high voluntary wheel running. J. Exp. Biol. 212:238–248.

Gray, A. A. 1907. The labyrinth of animals. Churchill, Lond.

———. 1908. The labyrinth of animals. Churchill, Lond.

Grossman, G. E., R. J. Leigh, L. A. Abel, D. J. Lanska, and S. E. Thurston. 1988. Frequency and velocity of rotational head perturbations during locomotion. Exp. Brain Res. 70:470–476.

Gunz, P., M. Ramsier, M. Kuhrig, J.-J. Hublin, and F. Spoor. 2012. The mammalian bony labyrinth reconsidered, introducing a comprehensive geometric morphometric approach. J. Anat. 220:529–543.

Hallgrímsson, B., D. E. Lieberman, W. Liu, A. F. Ford-Hutchinson, and F. R. Jirik. 2007. Epigenetic interactions and the structure of phenotypic variation in the cranium. Evol. Dev. 9:76–91.

Hassell, E. M. A., P. J. Meyers, E. J. Billman, J. E. Rasmussen, and M. C. Belk. 2012. Ontogeny and sex alter the effect of predation on body shape in a livebearing fish: sexual dimorphism, parallelism, and costs of reproduction. Ecol. Evol. 2:1738–1746.

Hayden, E. J., C. Weikert, and A. Wagner. 2012. Directional selection causes decanalization in a group I ribozyme. PLoS One 7:e45351.

Hirasaki, E., S. T. Moore, T. Raphan, and B. Cohen. 1999. Effects of walking velocity on vertical head and body movements during locomotion. Exp. Brain Res. 127:117–130.

Houle-Leroy, P., H. Guderley, J. G. Swallow, and T. Garland Jr. 2003. Artificial selection for high activity favors mighty mini-muscles in house mice. Am. J. Physiol. Regul. Integr. Comp. Physiol. 284:R433–R443.

Hoyte, D. A. N. 1961. The postnatal growth of the ear capsule in the rabbit. Am. J. Anat. 108:1–16.

Hullar, T. A. 2006. Semicircular canal geometry, afferent sensitivity and animal behavior. Anat. Rec. A Discov. Mol. Cell. Evol. Biol. 288:466–472.

Janvier, P. 2007. Evolutionary biology: born-again hagfishes. Nature 446:622–623.

Jeffery, N., and F. Spoor. 2004. Prenatal growth and development of the modern human labyrinth. J. Anat. 204:71–92.

Jones, G. M., and K. E. Spells. 1963. A theoretical and comparative study of the functional dependence of the semicircular canal upon its physical dimensions. Proc. R. Soc. Lon. B Biol. Sci. 157:403–419.

Kelly, S. A., P. P. Czech, J. T. Wight, K. M. Blank, and T. Garland Jr. 2006. Experimental evolution and phenotypic plasticity of hindlimb bones in high-activity house mice. J. Morphol. 267:360–374.

Kelly, S. A., T. M. Panhuis, and A. M. Stoehr. 2012. Phenotypic plasticity: molecular mechanisms and adaptive significance. Comprehensive Physiology 2:1417–1143.

Kelly, S. A., T. A. Bell, S. R. Selitsky, R. J. Buus, K. Hua, G. M. Weinstock, T. Garland Jr., F. P.-M. D. Villena, and D. Pomp. 2013. A novel intronic SNP in the *myosin heavy polypeptide 4* gene is responsible for the mini-muscle phenotype characterized by major reduction in hindlimb muscle mass in mice. Genetics 195:1385–1395.

Klingenberg, C. P. 2010. Evolution and development of shape: integrating quantitative approaches. Nat. Rev. Genet. 11:623–635.

———. 2011. MorphoJ: an integrated software package for geometric morphometrics. Mol. Ecol. Res. 11:353–357.

Kolb, E. M., E. L. Rezende, L. Holness, A. Radtke, S. K. Lee, A. Obenaus, and T. Garland Jr. 2013. Mice selectively bred for high voluntary wheel running have larger midbrains: support for the mosaic model of brain evolution. J. Exp. Biol. 216:515–523.

Koteja, P., T. Garland Jr., J. K. Sax, J. G. Swallow, and P. A. Carter. 1999. Behaviour of house mice artificially selected for high levels of voluntary wheel running. Anim. Behav. 58:1307–1318.

Langerhans, R. B. 2009. Trade-off between steady and unsteady swimming underlies predator-driven divergence in *Gambusia affinis*. J. Evol. Biol. 22:1057–1075.

Langerhans, R. B., and A. M. Makowicz. 2009. Shared and unique features of morphological differentiation between predator regimes in *Gambusia caymanensis*. J. Evol. Biol. 22:2231–2242.

Lasker, D., G. Han, H. Park, and L. Minor. 2008. Rotational responses of vestibular–nerve afferents innervating the semicircular canals in the c57bl/6 mouse. J. Assoc. Res. Otolaryngol. 9:334–348.

Lebrun, R., M. P. D. León, P. Tafforeau, and C. Zollikofer. 2010. Deep evolutionary roots of strepsirrhine primate labyrinthine morphology. J. Anat. 216:368–380.

Liao, D. 2013. Vectorized lab mouse mg 3263 for scientific figures and presentations. Pp. color mouse *in* Vectorized_lab_mouse_mg_3263_for_scientific_figures_and_presentations. svg, ed. wikimedia commons, http://commons.wikimedia.org/.

Lieberman, D. E., B. Hallgrímsson, W. Liu, T. E. Parsons, and H. A. Jamniczky. 2008. Spatial packing, cranial base angulation, and craniofacial shape variation in the mammalian skull: testing a new model using mice. J. Anat. 212:720–735.

Lieberman, D. E., D. M. Bramble, D. A. Raichlen, and J. J. Shea. 2009. Brains, brawn, and the evolution of human endurance running capabilities. Pp. 77–92 *in* F. E. Grine, J. G. Fleagle, and R. E. Leakey, eds. The first humans: origin and early evolution of the genus Homo. Springer, The Netherlands.

Lim, D. J., and M. Anniko. 1985. Developmental morphology of the mouse inner ear: a scanning electron microscopic observation. Acta Otolaryngol. 99:5–69.

Macrini, T. E., J. J. Flynn, D. A. Croft, and A. R. Wyss. 2010. Inner ear of a notoungulate placental mammal: anatomical description and examination of potentially phylogenetically informative characters. J. Anat. 216:600–610.

Malisch, J. L., C. W. Breuner, E. M. Kolb, H. Wada, R. M. Hannon, M. A. Chappell, K. M. Middleton, and T. Garland Jr. 2009. Behavioral despair and home-cage activity in mice with chronically elevated baseline corticosterone concentrations. Behav. Genet. 39:192–201.

Mazan, S., D. Jaillard, B. Baratte, and P. Janvier. 2000. Otx1 gene-controlled morphogenesis of the horizontal semicircular canal and the origin of the gnathostome characteristics. Evol. Dev. 2:186–193.

Middleton, K. M., S. A. Kelly, and T. Garland Jr. 2008a. Selective breeding as a tool to probe skeletal response to high voluntary locomotor activity in mice. Integr. Comp. Biol. 48:394–410.

Middleton, K. M., C. E. Shubin, D. C. Moore, P. A. Carter, T. Garland Jr., and S. M. Swartz. 2008b. The relative importance of genetics and phenotypic plasticity in dictating bone morphology and mechanics in aged mice: evidence from an artificial selection experiment. Zoology 111:135–147.

Middleton, K. M., B. D. Goldstein, P. R. Guduru, J. F. Waters, S. A. Kelly, S. M. Swartz, and T. Garland Jr. 2010. Variation in within-bone stiffness measured by nanoindentation in mice bred for high levels of voluntary wheel running. J. Anat. 216:121–131.

Monteiro, L. R. 1999. Multivariate regression models and geometric morphometrics: the search for causal factors in the analysis of shape. Syst. Biol. 48:192–199.

Morsli, H., D. Choo, A. Ryan, R. Johnson, and D. K. Wu. 1998. Development of the mouse inner ear and origin of its sensory organs. J. Neurosci. 18:3327–3335.

Mulavara, A. P., and J. J. Bloomberg. 2003. Identifying head-trunk and lower limb contributions to gaze stabilization during locomotion. J. Vestib. Res. 12:255–269.

Pélabon, C., T. F. Hansen, A. J. R. Carter, and D. Houle. 2010. Evolution of variation and variability under fluctuationg, stabilizing, and disruptive selection. Evolution 64:1912–1925.

Pozzo, T., A. Berthoz, and L. Lefort. 1990. Head stabilization during various locomotor tasks in humans. Exp. Brain Res. 82:97–106.

Rezende, E. L., and J. A. F. Diniz-Filho. 2012. Phylogenetic analyses: comparing species to infer adaptations and physiological mechanisms. Comp. Physiol. 2:639–674.

Rezende, E. L., M. A. Chappell, F. R. Gomes, J. L. Malisch, and T. Garland Jr. 2005a. Maximal metabolic rates during voluntary exercise, forced exercise, and cold exposure in house mice selectively bred for high wheel-running. J. Exp. Biol. 208:2447–2458.

———. 2005b. Maximal metabolic rates during voluntary exercise, forced exercise, and cold exposure in house mice selectively bred for high wheel-running. J. Exp. Biol. 208:2447–2458.

Rezende, Enrico L., F. R. Gomes, Mark A. Chappell, and T. Garland Jr. 2009. Running behavior and its energy cost in mice selectively bred for high voluntary locomotor activity. Physiol. Biochem. Zool. 82:662–679.

Ross, C. F., and M. J. Ravosa. 1993. Basicranial flexion, relative brain size, and facial kyphosis in nonhuman primates. Am. J. Phys. Anthropol. 91:305–324.

Ryan, T. M., M. T. Silcox, A. Walker, X. Mao, D. R. Begun, B. R. Benefit, P. D. Gingerich, M. Köhler, L. Kordos, M. L. McCrossin, et al. 2012. Evolution of locomotion in Anthropoidea: the semicircular canal evidence. Proc. R. Soc. B Biol. Sci. 279:3467–3475.

Sánchez-Villagra, M. R., and T. Schmelzle. 2007. Anatomy and development of the bony inner ear in the woolly opossum, *Caluromys philander* (Didelphimorphia, Marsupalia). Mastozoología Neotropical 14: 53–60.

Silcox, M. T., J. I. Bloch, D. M. Boyer, M. Godinot, T. M. Ryan, F. Spoor, and A. Walker. 2009. Semicircular canal system in early primates. J. Hum. Evol. 56:315–327.

Sørensen, M. S., P. Bretlau, and M. B. Jørgensen. 1990a. Bone modeling in the otic capsule of the rat. Acta Otolaryngol. 110:374–378.

———. 1990b. Quantum type bone remodeling in the otic capsule of the pig. Acta Otolaryngol. 110:217–223.

———. 1992. Bone repair in the otic capsule of the rabbit. Acta Otolaryngol. 112:968–975.

Sørensen, M. S., M. B. Jørgensen, and P. Bretlau. 1991. Remodeling patterns in the bony otic capsule of the dog. Ann. Otol. Rhinol. Laryngol. 100:751–758.

Spoor, F. 2003. The semicircular canal system and locomotor behaviour, with special reference to hominin evolution. Cour. Forsch-Inst. Senckenberg 243:93–104.

Spoor, F., and F. Zonneveld. 1995. Morphometry of the primate bony labyrinth: a new method based on high-resolution computed tomography. J. Anat. 186:271–286.

———. 1998. Comparative review of the human bony labyrinth. Am. J. Phys. Anthropol. 107:211–251.

Spoor, F., B. Wood, and F. Zonneveld. 1994. Implications of early hominid labyrinthine morphology for evolution of human bipedal locomotion. Nature 369:645–648.

———. 1996. Evidence for a link between human semicircular canal size and bipedal behaviour. J. Hum. Evol. 30:183–187.

Spoor, F., T. Garland, G. Krovitz, T. M. Ryan, M. T. Silcox, and A. Walker. 2007. The primate semicircular canal system and locomotion. Proc. Natl. Acad. Sci. USA 104:10808–10812.

Swallow, J. G., P. A. Carter, and T. Garland Jr. 1998. Artificial selection for increased wheel-running behavior in house mice. Behav. Genet. 28:227–237.

Swallow, J. G., P. Koteja, P. A. Carter, and T. Garland Jr. 1999. Artificial selection for increased wheel-running activity in house mice results in decreased body mass at maturity. J. Exp. Biol. 202:2513–2520.

Swartz, S. M., P. W. Freeman, and E. F. Stockwell. 2003. Ecomorphology of bats: comparative and experimental approaches relating structural design to ecology. Pp. 257–300 *in* T. H. Kunz and M. B. Fenton, eds. Bat ecology. University of Chicago Press, Chicago.

Syme, D. A., K. Evashuk, B. Grintuch, E. L. Rezende, and T. Garland. 2005. Contractile abilities of normal and "mini" triceps surae muscles from mice (Mus domesticus) selectively bred for high voluntary wheel running. J. Appl. Physiol. 99:1308–1316.

Takahashi, M., I. Akiyama, and N. Tsujita. 1989. Failure of gaze stabilization under high-frequency head oscillation. Acta Otolaryngol. 107:166–170.

Vidal, P.-P., L. Degallaix, P. Josset, J.-P. Gasc, and K. E. Cullen. 2004. Postural and locomotor control in normal and vestibularly deficient mice. J. Physiol. 559:625–638.

Walker, A., T. M. Ryan, M. T. Silcox, E. L. Simons, and F. Spoor. 2008. The semicircular canal system and locomotion: the case of extinct lemuroids and lorisoids. Evol. Anthropol. 17:135–145.

Wallace, I. J., S. M. Tommasini, S. Judex, T. Garland Jr., and B. Demes. 2012. Genetic variations and physical activity as determinants of limb bone morphology: an experimental approach using a mouse model. Am. J. Phys. Anthropol. 148:24–35.

Watt, H. J. 1924. Dimensions of the labyrinth correlated. Proc. R. Soc. Lond. B Biol. Sci. 96:334–338.

Wesner, J. S., E. J. Billman, A. Meier, and M. C. Belk. 2011. Morphological convergence during pregnancy among predator and nonpredator populations of the livebearing fish *Brachyrhaphis rhabdophora* (Teleostei: Poeciliidae). Biol. J. Linn. Soc. 104:386–392.

Yang, A., and T. E. Hullar. 2007. Relationship of semicircular canal size to vestibular-nerve afferent sensitivity in mammals. J. Neurophysiol. 98:3197–3205.

Young, N., B. Hallgrímsson, and T. Garland Jr. 2009. Epigenetic effects on integration of limb lengths in a mouse model: selective breeding for high voluntary locomotor activity. Evol. Biol. 36:88–99.

Zehnder, A. F., A. G. Kristiansen, J. C. Adams, S. N. Merchant, and M. J. McKenna. 2005. Osteoprotegerin in the inner ear may inhibit bone remodeling in the otic capsule. Laryngoscope 115: 172–177.

Zehnder, A. F., A. G. Kristiansen, J. C. Adams, S. G. Kujawa, S. N. Merchant, and M. J. McKenna. 2006. Osteoprotegrin knockout mice demonstrate abnormal remodeling of the otic capsule and progressive hearing loss. Laryngoscope 116:201–206.

Associate Editor: P. David Polly

Supporting Information

Additional Supporting Information may be found in the online version of this article at the publisher's website:

Appendix S1. Data collection of mice from selectively bred lines
Appendix S2. μCT scans, linear measurements and data analysis
Appendix S3. 3D landmarks and centroid size
Appendix S4. Body mass and size metrics used
Appendix S5. Anatomical description of morphological differences
Table S1. Anatomical description of 3D landmarks.
Table S2. Means and standard errors of the mean for body mass and canal radius of curvature.
Animation S1. Animation of deformations in semicircular canal shape along Principal component (PC) 1.
Animation S2. Animation of deformations in semicircular canal shape along Principal component (PC) 2.

Supplementary Materials for

SHAPE-SHIFT: SEMICIRCULAR CANAL MORPHOLOGY RESPONDS TO SELECTIVE BREEDING FOR INCREASED LOCOMOTOR ACTIVITY

Heidi Schutz[1,2*], Heather A. Jamniczky[3], Benedikt Hallgrímsson[3], Theodore Garland, Jr.[2]

[1] Biology Department, Pacific Lutheran University, Tacoma, WA 98477, USA
[2] Department of Biology, University of California, Riverside, CA 92521, USA
[3] McCaig Institute for Bone and Joint Health, Department of Cell Biology & Anatomy, Cumming School of Medicine , University of Calgary Calgary, Alberta T2N 4N1, Canada
*address for correspondence:

Heidi Schutz, Biology Department, Pacific Lutheran University, Tacoma, WA 98477, USA
Phone: 253-535-7094; Fax: 253-536-7561; Email: schutzha@plu.edu

CONTENTS OF SUPPLEMENTARY MATERIALS

SUPPLEMENTARY METHODS

Appendix S1: Data Collection of Mice from Selectively Bred Lines 3
Appendix S2: µCT Scans, Linear Measurements and Data Analysis 5
Appendix S3: 3D Landmarks and Centroid size 6
Table S1: Anatomical Description of 3D Landmarks 8
Appendix S4: Body Mass and Size Metrics Used 10

SUPPLEMENTARY RESULTS

Table S2: Means and standard errors 11
Appendix S5: Anatomical description of morphological differences 12
Animation S1 13
Animation S2 13

LITERATURE CITED **14**

SUPPLEMENTARY METHODS

Appendix S1: Data Collection of Mice from Selectively Bred Lines

Detailed descriptions of the experimental design, rationale, and protocols for the long-term selection experiment are described in greater detail elsewhere (Swallow et al. 1998; Garland 2003; Careau et al. 2013), and we provide a summary of the relevant aspects of the selection experiment below.

Eight closed lines of 10 mating pairs each were established from a founder population of 224 outbred ICR strain mice (Harlan Sprague Dawley, Indianapolis, IN) which were randomly mated for two generations before establishing the lines. At random, four of the eight lines were designated as non-selected controls (C), and the other four were designated as high runner (HR) lines in which the parents of subsequent generations are those mice that exhibit the highest levels of voluntary wheel running during the 5th and 6th days of a 6-day exposure to Wahman-type running wheels measuring 1.12m in circumference. Each mouse is placed in a home-cage connected to a running wheel (which they can enter and exit at will) at 6-8 weeks of age, and their voluntary wheel running activity is monitored via an automated system. In the HR lines, the males and females with the highest number of total revolutions on days 5 and 6 in each family (10 in each line) are chosen as breeders. For both the HR and C lines, all breeding pairs are chosen at random from each family and no sibling or cross-line or line-type matings are allowed.

Results of analyses of the long bone skeletal components of the hind limb in this mouse sample from generation 21 are described in Kelly et al. (2006), which also provides a more comprehensive description of the specific experimental protocol and rationale. What follows, is a brief summary.

Because of sex differences in body size and wheel running, only males were chosen for this experiment. Five families within each of the eight experimental lines in generation 20 were allowed to produce a second litter and male sibling pups from these second litters of generation 21 (n= 80) populated the experiment. Individuals were weaned at 21 days of age and at 25-28 days old, mice were individually housed in standard cages and assigned to a wheel access or no wheel access treatment group for 8-9 weeks by blocking or allowing access to wheels. At an average age of 85.6 days, mice were sacrificed by CO_2 and whole body morphometrics (nose -rump length and body mass) were obtained immediately after sacrifice, then various organs were dissected. Carcasses were then stored frozen and later skeletonized using a dermestid colony. All procedures conformed to guidelines established by the Institutional Animal Care and Use Committee at the University of Wisconsin-Madison.

Ultimately, the sample sizes for all treatment groups in this study were as follows: two male siblings from each of five families per line. Each sibling was then placed in either the wheel access or no wheel access group producing 10 representative individuals per line, half with wheels and half without. Of the 40 C–line individuals, none were identified as having the mini-muscle phenotype. Of the 40 HR individuals, nine exhibited the mini-muscle phenotype with three in line 3 (two housed with wheels, one without) and six in line 6 (three housed with wheels, three without).

Appendix S2: μCT Scans, Linear Measurements and Data Analysis

Temporal cranial regions were scanned under the following parameters: (55kv, 145μA, 500 projections). Individual scans were loaded into the Amira® 5.0 software platform (Visualization Sciences Group, Burlington, MA) (Visage Imaging, San Diego, CA) for visualization, semicircular canal endocast reconstruction, linear measurements, and 3D landmarking.

When calculating the radius of curvature (R) R= 0.5 X (height + width)/2 sensu (Curthoys et al. (1977), measurement error was mitigated by measuring the heights and widths of each canal three times and averaged to produce an average height and width. These means were then used to calculate radius of curvature.

Appendix S3: 3D Landmarks and Centroid Size

The three dimensional landmarking protocol in Amira was performed as follows: First, using the AutoSkeleton module, we applied a thinning algorithm to reduce the data to a string of connected centerline voxels traversing the cochlea, vestibule, and all three semicircular canals. This computed midline scaffold (Fig. 1) facilitated consistent landmark placement by delineating points of intersection (e.g. the point at which the superior and posterior canal converge on a single structure at landmark 1) more clearly and by assisting in the consistent placement of some of semi-landarks such as those located in the center of the lumen of each canal (i.e. 2, 6 and 10 at landmarks at the ampullae).

This landmarking scheme differs from that recently employed by Gunz et al. (2012), who used a semi-landmark based method designed to accommodate the large amount of variation in their sample produced by their broad phylogenetic comparison. In the present study however, landmark homology is obviously less problematic because our comparisons were performed within a species rather than among species.

Once 3D landmarks were acquired, information related to position, rotation, and scaling was removed using generalized least-squares Procrustes superimposition, in order to extract geometric shape variation for all individuals in the sample (Dryden and Mardia 1998). This procedure yields Procrustes shape coordinates lacking variation due to scale differences but including allometric variation in shape. Centroid size, the sum of the squared distances from each landmark to the centroid, was also calculated for each specimen. Finally, the principal components (PCs) of shape were calculated from a principal component analysis (PCA) of the variance–covariance matrix of the Procrustes coordinates, following standard geometric morphometric techniques (Dryden and Mardia 1998). In addition to

generating the multivariate descriptors of shape, we also assessed whether size adjustment of the shape data before analysis was appropriate. To do so, we performed a pooled-within group multivariate regression of shape on centroid size in MorphoJ (ver 1.03a) software package (Klingenberg 2011). The result was statistically significant (P=0.004), suggesting that the overall size of all three semicircular canals as measured by centroid size has a significant effect on canal shape. The regression residuals were then used as size-corrected shape data (recall that this is size correction for the size of the canals and not a correction based on body size) and used in the full analyses. All results of these analyses showed similar patterns to analyses performed on the non-adjusted data, but with reduced levels of statistical significance (larger P values).

Table S1: Anatomical Description of 3D Landmarks**.** Three dimensional landmarks representing all three semicircular canals with 12 of the 14 total landmarks derived from Lebrun et al. (Lebrun et al. 2010) and identified as such by an *. All landmarks are also shown in Figure 1.

Landmark number	Anatomical description
1*	Bifurcation point of the common crus between the anterior and posterior canals.
2*	Centre of the ampulla of the lateral semicircular canal
3*	Posteromedial-most point at the centre of the lumen of the lateral semicircular canal.
4*	Posterolateral-most point at the centre of the lumen of the lateral semicircular canal. *Effectively at the apex of the lateral canal.*
5*	Anterolateral-most point at the centre of the lumen of the lateral semicircular canal.
6*	Center of the ampulla of the anterior semicircular canal.
7*	Anterolateral-most point at the centre of the lumen of the anterior semicircular canal.
8*	Superior-most point at the centre of the lumen of the anterior semicircular canal. *Effectively at the "apex" of the anterior canal.*
9	Inferior-most point at the junction of the common crus and the vestibule in the posterior semicircular canal plane. This point also covers the junction of the lateral canal with the vestibule.
10*	Center of the ampulla of the posterior semicircular canal

11*	Inferior-most point at the center of the lumen of the posterior semicircular canal.
12*	Superior-most point at the centre of the lumen of the posterior semicircular canal. *Effectively at the "apex" of the posterior canal.*
13*	Posterolateral-most point at the centre of the lumen of the posterior semicircular canal
14	Inferior-most point at the junction of the common crus and the vestibule in the anterior semicircular canal plane.

Appendix S4: Body Mass and Size Metrics used

This dataset generated many size metrics and it was important to determine which one was most appropriate for inclusion into the final analyses. First we began by testing for correlations between size metrics. As expected, all size metrics were intercorrelated. Centroid size was highly correlated with average semicircular canal radius of curvature (n= 80, $r = 0.864$, $P < 0.001$) and moderately correlated with body mass ($r = 0.369$, $P < 0.001$), whereas canal radius of curvature and body mass were also correlated ($r = 0.360$, $P < 0.001$).

We then performed follow-up multivariate multiple regressions of the entire set of Procrustes coordinates describing semicircular canal shape against both centroid size and body mass in order to assess the allometric effects of size (Bookstein 1991; Mitteroecker et al. 2004). These analyses demonstrated a strong allometric component to shape, and the multivariate multiple regression using centroid size as an independent variable showed that centroid size explains 71.2% of the variation in canal shape ($P < 0.001$). The multivariate multiple regression using body mass showed that allometry explains 63.8% of the variation in canal shape and is also statistically significant ($P < 0.001$).

Given these results, we did not use centroid size, average radius of curvature, and body mass in the same model and we chose to report the results of all subsequent analyses with body mass as the relevant size measure for three reasons. First, our analyses using body mass were more comparable to those in previous studies of semicircular canal size and shape. Second, results utilizing other size measures were comparable to the results using body mass. Third, because centroid size likely encompasses both body size and canal size, its inclusion is redundant and statistically problematic.

SUPPLEMENTARY RESULTS

Table S2: Means and standard errors of the mean for body mass and canal radius of curvature. For ANCOVA results, see main text.

	Control lines				**HR lines**				**Mini-Muscle**			
	No Wheels		Wheels		No Wheels		Wheels		No Wheels		Wheels	
Trait	Mean	SE	Mean	SE	Mean	SE	Mean	SE	Mean	SE	Mean	SE
Body Mass (g)	33.8	0.82	32.5	0.82	29.6	0.71	28.3	0.69	32.1	0.44	30	0.98
R of the anterior canal (mm)	0.8172	0.00530	0.8271	0.00428	0.8077	0.00768	0.8046	0.00886	0.7954	0.1115	0.8087	0.01637
R of the lateral canal(mm)	0.5968	0.00482	0.5925	0.00052	0.5874	0.00542	0.5859	0.00716	0.5796	0.00933	0.5975	0.1284
R of the posterior canal (mm)	0.6918	0.01044	0.6948	0.00906	0.6900	0.00612	0.6866	0.00574	0.6848	0.01018	0.6858	0.1094
Mean R for all three canals (mm)	0.7019	0.00583	0.7048	0.00545	0.6950	0.00564	0.6924	0.00611	0.6866	0.00787	0.6973	0.01232

Appendix S5: Anatomical Description of Morphological Differences

Semicircular canal shape differences, as represented by the PC axes (particularly axes 1-3, see Fig. 3 and Animations S1 and S2), occur primarily in the position of the canals and ampullae relative to one another, as well as differences in the degree of co-planarity of the canals. For two of the three axes described (PC 1 and 2), HR individuals primarily lie in the negative shape space and C individuals lie in the positive shape space, whereas for PC 3, HR individuals primarily lie in the positive shape space and C individuals in the negative. Along PC 1 (see also the supplementary video showing the shape changes along this axis), individuals in the negative shape space (primarily HR and shown in red in Fig. 3) have anterior canals with antero-lateral torsion, posterior canals with anterior displacement, and lateral canals with slight infero-superior torsion and displacement relative to individuals in the positive shape space (primarily C and shown in the black model). Along PC 2 (see also the supplementary video showing the shape changes along this axis), individuals in the negative shape space (primarily HR and shown in red in Fig. 3) have anterior canals that are more medio-laterally coplanar and medially displaced, posterior canals that are more postero-anteriorly coplanar and posteriorly displaced, and lateral canals that are more supero-inferiorly coplanar relative to individuals in the positive shape space (primarily C and shown in the black model). Finally, along PC 3, individuals in the positive shape space (primarily HR and shown in red in Fig. 3) have anterior canals that are both medially displaced and have greater medio-lateral co-planarity, anteriorly displaced and antero-posteriorly curved posterior canals, and superiorly displaced but similarly co-planar lateral canals relative to individuals in the negative shape space (primarily C and shown in the black model).

Animation S1 (PC1_animation.avi). Animation of deformations in semicircular canal shape along Principal component (PC) 1. For a dataset of 80 mice, PC 1 explains 18.3% of the total shape variation and the animation depicts changes in shape along PC1 from the negative region (primarily depicting HR semicircular canal morphology) to the positive region (primarily depicting C canal morphology). Thus, the animation shows shifts in shape from primarily HR individuals at the beginning, to C individuals at the end.

Animation S2 (PC2_animation.avi). Animation of deformations in semicircular canal shape along Principal component (PC) 2. For a dataset of 80 mice, PC 2 explains 14.2% of the total shape variation and the animation depicts changes in shape along PC2 from the negative region (primarily depicting C semicircular canal morphology) to the positive region (primarily depicting HR canal morphology). Thus, the animation shows shifts in shape from primarily C individuals at the beginning, to HR individuals at the end.

LITERATURE CITED

Bookstein, F. L. 1991. Morphometric tools for landmark data: Geometry and biology. Cambridge University Press, New York.

Careau, V., M. E. Wolak, P. A. Carter, and T. Garland. 2013. Limits to behavioral evolution: the quantitative genetics of a complex trait under directional selection. Evolution 67:3102-3119.

Curthoys, I. S., R. H. I. Blanks, and C. H. Markham. 1977. Semicircular canal radii of curvature (R) in cat, guinea pig and man. Journal of Morphology 151:1-15.

Dryden, I. L. and K. V. Mardia. 1998. Statistical shape analysis: Wiley series in probability and statistics. John Wiley & Sons, Ltd, New York.

Garland, T., Jr. 2003. Selection experiments: an under-utilized tool in biomechanics and organismal biology. Pp. 23-56 *in* V. L. Bels, J.-P. Gasc, and A. Casinos, eds. Vertebrate Biomechanics and Evolution Oxford.

Garland, T., Jr., M. T. Morgan, J. G. Swallow, J. S. Rhodes, I. Girard, J. G. Belter, and P. A. Carter. 2002. Evolution of a small-muscle polymorphysm in lines of house mice selected for high activity levels. Evolution 56:1267-1275.

Gunz, P., M. Ramsier, M. Kuhrig, J.-J. Hublin, and F. Spoor. 2012. The mammalian bony labyrinth reconsidered, introducing a comprehensive geometric morphometric approach. Journal of Anatomy 220:529-543.

Houle-Leroy, P., H. Guderley, J. G. Swallow, and T. Garland, Jr. 2003. Artificial selection for high activity favors mighty mini-muscles in house mice. American Journal of Physiology - Regulatory, Integrative and Comparative Physiology 284:R433-R443.

Kelly, S. A., P. P. Czech, J. T. Wight, K. M. Blank, and T. Garland, Jr. 2006. Experimental evolution and phenotypic plasticity of hindlimb bones in high-activity house mice. Journal of Morphology 267:360-374.

Klingenberg, C. P. 2011. MorphoJ: an integrated software package for geometric morphometrics. Molecular Ecology Resources 11:353-357.

Lebrun, R., M. P. d. León, P. Tafforeau, and C. Zollikofer. 2010. Deep evolutionary roots of strepsirrhine primate labyrinthine morphology. Journal of Anatomy 216:368-380.

Middleton, K. M., S. A. Kelly, and T. Garland, Jr. 2008. Selective breeding as a tool to probe skeletal response to high voluntary locomotor activity in mice. Integrative and Comparative Biology 48:394-410.

Mitteroecker, P., P. Gunz, M. Bernhard, K. Schaefer, and F. L. Bookstein. 2004. Comparison of cranial ontogenetic trajectories among great apes and humans. Journal of Human Evolution 46:679-698.

Swallow, J. G., P. A. Carter, and T. Garland, Jr. 1998. Artificial selection for increased wheel-running behavior in house mice. Behav. Genet. 28:227-237.